Circulation Research

JOURNAL OF THE AMERICAN HEART ASSOCIATION

Manuscript Number: CIRCRESAHA/2010/217224

Article Type: Regular Article

Title: Impact of competitive flow on wall shear stress in coronary surgery: Computational fluid dynamics of a LIMA-LAD anastomosis in a 3-D porcine model

Authors: Håvard B. Nordgaard, Abigail Swillens, Dag Nordhaug, Idar Kirkeby-Garstad, Denis Van Loo, Nicola Vitale, Patrick Segers, Rune Haaverstad, and Lasse Løvstakken

Circulation Research Online Submission: http://submit-circres.ahajournals.org
Circulation Research Homepage: http://circres.ahajournals.org
Circulation Research Editorial Office
3355 Keswick Rd, Main Bldg 103
Baltimore, MD 21211
circulation.research@circresearch.com
Telephone: 410-327-5005
Fax: 410-327-9322

Impact of competitive flow on wall shear stress in coronary surgery: Computational fluid dynamics of a LIMA-LAD anastomosis in a 3-D porcine model

Nordgaard – Impact of competitive flow on shear stress in CABG

Håvard Nordgaard, MD[1,2]; Abigail Swillens, MScEng [3]; Dag Nordhaug, MD PhD[1,2]; Idar Kirkeby-Garstad, MD PhD[1,2]; Denis Van Loo, MScEng[5]; Nicola Vitale, MD PhD[2]; Patrick Segers, MScEng PhD[3], Rune Haaverstad, MD PhD[1,4]; Lasse Løvstakken, MScEng PhD [1]

[1]Dept.of Circulation and Medical Imaging, The Norwegian University of Science and Technology, Trondheim, Norway; [2]Dept. of Cardiothoracic Surgery, St. Olavs University Hospital, Trondheim, Norway; [3]Institute Biomedical Technology, Ghent University, Belgium; [4]Dept. of Surgical Sciences, University of Bergen, Norway; [5]UGCT-Centre for X-ray Tomography of Ghent University, Belgium

Corresponding Author: Håvard Nordgaard MD
Department of Circulation and Medical Imaging,
Norwegian University of Science and Technology
N-7489 Trondheim, Norway
Tel (+47) 91717994 / Fax (+47) 73867029
E-mail: haavardnordgaard@gmail.com

Word count: 5200

Subject codes: [36]; [95]; [97]; [134]; [135]

Abstract

Rationale: Low and oscillatory wall shear stress (WSS) on the endothelial surface is a major determinant of endothelial dysfunction and may play an important role in graft failure after coronary artery bypass grafting (CABG). Competitive flow from native coronary vessels is considered a major factor in the narrowing and long-term failure of grafts, including the mammary artery.

Objective: To investigate the impact of competitive flow on WSS in mammary grafts.

Methods and Results: Using computational fluid dynamics, WSS was calculated in a left internal mammary artery graft to the left anterior descending artery in a 3-D *in vivo* porcine model of CABG. The following conditions were investigated: 1) high competitive flow (non-significant coronary lesion), 2) partial competitive flow (significant coronary lesion), and 3) no competitive flow (totally occluded coronary vessel). Time-averaged WSS for each case ranged as follows: 1) 0.3-0.5 Pa, 2) 0.6-3.0 Pa, and 3) 0.9-3.0 Pa, respectively. Further, oscillatory WSS quantified as the oscillatory shear index (OSI) ranged from (maximum OSI = 0.5 equals zero net WSS): 1) 0.15-0.35, 2) <0.05, and 3) <0.05, respectively. Thus, high competitive flow resulted in substantial oscillatory and low WSS in the LIMA. Moderate competitive flow resulted in WSS and OSI similar to the no-competitive flow condition.

Conclusions: Graft flow is highly dependent on the degree of competitive flow. High competitive flow was found to produce unfavourable WSS conditions consistent with endothelium dysfunction and subsequent graft narrowing and failure. Partial competitive flow however, may be better tolerated as it was found to be similar to the ideal condition of no competitive flow.

Keywords: CABG, competitive flow, wall shear stress (WSS), graft patency

Non-standard Abbreviations and Acronyms:

CFD	Computational fluid dynamics
LAD	Left anterior descending artery
LIMA	Left internal mammary artery
OSI	Oscillatory shear index
WSS	Wall shear stress

Introduction

Wall shear stress (WSS) may play an important role in graft patency after coronary artery bypass surgery [1]. Several reports provide substantial evidence on the impairment of endothelial function due to WSS alterations [2-6]. The frictional shear force determined by blood flow impacting on the endothelium triggers a biochemical response, exerting a critical impact on endothelial function and structure as well as gene expression [4]. Genetic predisposition and several systemic factors (i.e., hypertension, diabetes mellitus, hypercholesterolemia, and smoking) exert a prominent influence on the progression of coronary artery disease [7]. However, the arterial lesions are mostly "site specific", signifying an interaction between the endothelial cells and the altered WSS occurring in critical areas. In detail, vessel areas with low and oscillatory (bidirectional) WSS, like the inner wall of curved segments and the outer wall of bifurcations, are considered non-optimal and more prone to endothelial dysfunction and vascular disease [1, 3-6, 8, 9]. On the other hand, vessel areas exposed to steady and unidirectional blood flow with a physiologically moderate-to-high WSS remain relatively disease-free [1, 3-6, 8, 9]. Moreover, Fukumoto et al. suggested that a very high WSS (i.e., > 7 Pa) may cause endothelial damage and promote plaque rupture, although this mechanism has not yet been fully elucidated [10].

Unfortunately, at present WSS cannot be measured directly in the vessels, but it can be estimated in models in which different fluid properties, such as viscosity and velocity, and geometric conditions, like inner vessel surface, are known. Nowadays computational fluid dynamics (CFD) is the most common method to explore complex flow mechanics and to investigate the WSS distribution in arteries, including native coronary arteries and bypass grafts [2, 11, 12].

The patency of coronary artery bypass grafts is mainly determined by the progression of atherosclerosis and intimal hyperplasia within the grafts as well as technical failures (i.e., anastomotic stenosis) [13]. There is substantial evidence that competitive flow is associated with graft failure, and it is considered to be one of the major factors resulting in the 10% long-term failure of the left internal mammary artery (LIMA) graft directed to the left anterior descending artery (LAD). Moreover, competitive flow is thought to determine the narrowing of the whole length of the LIMA graft, the so called "string phenomenon" [14-19]. Although, the negative impact of competitive flow on graft patency has been reported in several studies [14-19], the exact patho-physiological effects are not fully understood because most of these studies do not provide clear explanations for their findings.

The aim of the present study is a detailed assessment of the impact of competitive flow on WSS in a LIMA-to-LAD anastomosis model. The novelty of this study is the high accuracy of the input data used in the biomechanical simulations, derived *in vivo* from a porcine CABG model. In particular, a 3-D geometric model was created from a cast of the real anastomosis, and simultaneous transit-time flow curves were recorded in the LIMA and LAD.

Materials and methods

A Noroc pig (hybrid of ¼ Duroc, ¼ Yorkshire and ½ Norwegian landrace; weight 65 kg) underwent off-pump CABG with the LIMA to LAD anastomosis through a median sternotomy. The pig received good care in accordance with the European convention on animal care and Norwegian national regulations. Approval was given by the Norwegian Ethics Committee on animal research. At the completion of the experiments, the pig was sacrificed with an intravenous injection of high dose pentobarbital.

The pig received premedication with intramuscular azaperone 4 mg/ kg and ketamine 0.20 mg/kg. Anesthesia was induced with intravenous atropine 1 mg, fentanyl 0.01 mg/kg and pentobarbital 10 mg/kg. General anesthesia was maintained by infusions of fentanyl at 0.02 mg/kg/hour and midazolam 0.3 mg/kg/hour. Amiodarone 150 mg and hexamethonium chloride 20 mg/kg were given to avoid arrhythmias. Full heparinization was achieved with heparin 15 000 IE intravenously. The pig was ventilated with oxygen 40% in room air through a tracheotomy tube, and ventilator settings were adjusted according to blood gas measurements. Central venous catheters were introduced into both internal jugular veins for infusion and measurement of central venous pressure. A catheter was placed in the descending thoracic aorta for continuous measurement of arterial pressure. The bladder was drained through a cystotomy.

After median sternotomy, the LIMA was harvested with its pedicle. An Axius Vacuum Stabilizer (Guidant, Santa Clara, CA, USA) was applied to immobilize the LAD at the site chosen for grafting. Ischemic preconditioning was performed by five repeated cycles of 30 seconds of LAD occlusion with 30 seconds of reperfusion in between. After arteriotomy of the LAD, an intracoronary shunt was placed in the vessel lumen. The LIMA-LAD anastomosis was then performed with a continuous 7-0 polypropylene suture.

Epicardial ultrasound imaging, performed with a GE Vivid 7 scanner (GE Vingmed, Norway) equipped with a i13L linear array probe (GE Healthcare, WI, USA), was used to verify a patent anastomosis without technical failure, as well as for blood flow visualization for use in further qualitative validation of the biomechanical fluid simulations (Fig 3).

Pulsatile blood flow measurements of LIMA and LAD

The flow measurements needed as input for the 3-D computer model were obtained using a transit-time flowmeter (VeriQ, MediStim ASA, Norway). Simultaneous flow recordings were obtained at stable hemodynamic conditions (heart rate, cardiac output and blood pressure) under three different flow conditions as shown in Figure 1: 1) High competitive flow (non-significant coronary lesion), 2) partial competitive flow (significant coronary lesion), and 3) no competitive flow (totally occluded coronary vessel). Two 3-mm flow probes were placed around the LAD proximal to the anastomosis to assess the competitive flow and around the LIMA to record the graft flow. Adjacent to the flow probe on the LAD, an adjustable occluder (In Vivo Metric, CA, US) was applied to adjust the level of competitive flow. Simulation of non-significant and significant coronary stenosis was achieved by total and partial pressure release of the vascular occluder. The partial pressure release halved the LAD flow. Additionally, a 16-mm flow probe was placed around the pulmonary trunk to measure cardiac output and to differentiate systole from diastole.

Acquisition of the 3-D LIMA-to-LAD anastomosis model

The acquisition of the model was a three stage process as illustrated in Figure 2. After surgery and sacrifice of the pig, the heart was excised with its LIMA graft. The vessels were antegrade perfused with water until all blood was washed away. The cast of the LIMA - LAD anastomosis was created by injecting a resin of methyl methacrylate (Technovit 7143, Kulzer, Wehrheim, Germany). Once the resin solution stiffened completely, the tissue was removed with potassium hydroxide to fabricate a cast representing the lumen of the LAD, the LIMA and the anastomosis.

The 3-D volume of the cast was scanned using a high resolution micro-CT setup consisting of a Feinfocus transmission target (Yxlon, Hamburg, Germany), a Paxscan 2520 X-ray tube, a-Si flat panel detector with 127µm pixel pitch (Varian, UT, USA), and a UPR-160 air-bearing rotation stage (Micos, Eschbach, Germany). The resulting voxel pitch achieved was 17.7 µm.

Finally, the dataset of 1200 x 1200 x 1500 isotropic voxels was processed in Mimics (Materialise, Leuven, Belgium) for surface segmentation of the cast and to generate the simulation mesh, resulting in geometry consisting of a tetrahedral grid of 1,058,405 elements. The simulation mesh was adapted and improved using Magics (Materialise, Leuven, Belgium). For the sake of simplicity, the smaller septal and diagonal branches of the LAD in the original cast model were removed. In the end, the three major septal and two diagonal branches assumed to most influence the resulting flow patterns were included.

Computational Fluid Dynamics simulations

Computational fluid dynamics (CFD) uses numerical methods and algorithms to solve and analyze problems that involve fluid flows; in particular, the Navier-Stokes equations that govern the motion of fluids are used. *In vivo* flow fields can then be recreated in the computer based on a given 3-D geometric computer model and knowledge of flow conditions at the inlets and outlets, as for example measured flow curves. The input data used in this study were obtained by (1) the pulsatile volume flow curves measured using transit-time flowmetry as described above and (2) the 3-D model of the inner surface of the LIMA-LAD model obtained through micro-CT scanning of the anastomosis cast. The flow curves were averaged over ten cardiac cycles. The flow curves were further assumed to be the time varying maximum of a fully developed flow profile, and thus transformed into a parabolic velocity profile at the inlets. A non-slip condition at the vessel wall and full laminar flow was assumed. A fixed outflow division was further assumed for the distal LAD and the septal and diagonal branches of the LAD based on their relative cross sectional areas.

The commercial CFD software Fluent 6.2 (Ansys, PA, USA) was used to numerically solve the Navier-Stokes equations using a finite volume method. Blood was modeled as an incompressible Newtonian fluid with dynamic viscosity and density respectively set to 3.5 mPa·s and 1050 kg/m^3, and rigid walls were assumed. The Fluent CFD software assumed fully developed parabolic flow at outflow boundaries, and cylindrical extensions were therefore matched to the outlet surfaces to achieve this. The cardiac cycle was divided into 130 equally spaced time steps of 5 ms, and three cycles were computed to obtain results fully independent of any transient effects. Simulation wise, standard pressure discretization and second-order upwind momentum discretization were used, and the pressure-velocity coupling scheme was the semi-implicit method for pressure-linked equations (SIMPLE) algorithm.

Post processing, figure plotting, and analysis of CFD simulations were made in Tecplot (Tecplot Inc., WA, USA).

Definition of wall shear stress (WSS) and oscillatory shear index (OSI)

The WSS is the tangential frictional force on the endothelial surface. It is expressed in units of force/ unit area (Pascal [Pa] or dyne/cm^2; 1 Pa = 10 dyne/cm^2). The shear stress pattern is determined by the pulsatile flow in combination with the complex geometric structure of the vessels. For a Newtonian fluid, shear stress τ is proportional to the flow shear rate (the change in flow velocity across the vessel), and the dynamic blood viscosity μ, which for a straight vessel can be expressed as:

$$\tau = \mu \cdot \frac{\partial v}{\partial y},$$

where y and v are the distance and velocity parallel to the wall, respectively. The WSS is further defined as the shear stress at the vessel wall. For steady and laminar flow in a straight vessel (Poiseuille flow), the following equivalent form for WSS is given in terms of volume flow rate Q and inner vessel radius R:

$$\tau = \frac{4\mu Q}{\pi R^3}.$$

Thus, small changes in radius R greatly influence the shear stress τ. The WSS in normal arteries varies from 1 to 7 Pa, while atherosclerosis-prone regions exhibit from – 0.4 to 0.4 Pa. Non-physiologically high WSS however have been reported to be > 7 Pa, usually seen in severe stenosis, cardiac valves and stents [6].

The oscillatory shear index (OSI) is a measure which allows quantifying the change in direction and magnitude of the WSS, and it is calculated according to the following formula:

$$\mathrm{OSI} = \frac{1}{2} \cdot \left(1 - \frac{\left| \int_0^T \tau \, dt \right|}{\int_O^T |\tau| \, dt} \right),$$

where T is the time of a cardiac cycle and τ is the WSS vector [20]. The nominator and the denominator display the total WSS (the sum of all positive and negative WSS vectors) and the sum of all absolute values of the same WSS vectors over a cardiac cycle, respectively. It ranges from 0 to 0.5, where 0 describes a total unidirectional WSS and the latter a purely unsteady, oscillatory shear flow with a net amount of zero WSS. Areas of high OSI are predisposed to endothelial dysfunction and atherogenesis [4, 20].

Results

In Figure 3, a qualitative comparison between the predicted CFD flow field and the observed flow field from color-Doppler images acquired during surgery is provided for the case of high competitive flow. The directions and axial velocity magnitudes from CFD simulations corresponded well with the color-Doppler images both in systole and diastole.

The CFD simulations identified areas of wide variations of the WSS (approximate range 0.1 – 15 Pa). Figure 4 shows the time-average WSS mapping at low and high WSS-scale under the three experimental conditions. The high competitive flow resulting from a non-significant stenosis produced overall low WSS in the LIMA graft (Figure 4-C). On the other hand, partial competitive flow resulted in a WSS more similar to the no-competitive flow condition (Figure 4-A and 4-B). The mapping of WSS at the high WSS-scale showed the highest WSS levels in the LIMA graft at no-competitive flow conditions (Figure 4-A), whereas all three conditions produced similar high WSS values at the toe of the anastomosis (Figures 4 and 6).

Figure 5 represents the OSI mapping, showing a clear increase of OSI from the no- and partial competitive flow conditions to the high competitive flow condition, where high OSI can be observed.

The WSS variations throughout the cardiac cycle are dependent on flow velocities, with higher WSS at higher blood flow velocities. The highest WSS values in the LIMA graft were found during mid-systole and particularly in mid-diastole, the moment when the coronary and graft flow is at the highest (Figure 6). Substantially lower WSS values were found in areas of low flow, especially where retrograde and disturbed flows appear, typically seen during competitive flow conditions (Figures 4 and 6).

Discussion

The main results of this study are that different degrees of competitive flow in the coronary arteries determine different WSS distributions in the LIMA-to-LAD anastomosis. In detail, high competitive flow, as may occur in the presence of non-significant coronary stenosis, resulted in the lowest WSS and highest OSI both in the LIMA graft and the anastomosis. Partial competitive flow, as may occur in significant stenosis, produced a WSS distribution comparable to the ideal situation of no-competitive flow. These findings may have immediate and important application in clinical practice: the coronary graft is able to tolerate a modest degree of competitive flow without major alterations in WSS distribution. On the contrary, major competitive flow triggers a decrease in WSS that may impair graft patency in the long-term. These conclusions are in line with previous clinical studies addressing graft patency. Berger et al. reported that the degree of preoperative proximal coronary stenosis was a major predictor of mammary graft occlusion [15]. Several other authors reported better long-term patency of grafts when these were placed distal to severe stenoses [14, 16-19, 21, 22]. In another study by Shah et al., possible factors affecting graft patency were studied in 1482 LIMA grafts via angiography in symptomatic patients [23]. No relationship between the degree of native coronary stenosis and LIMA patency was found. However, an important limitation of the study was that native vessels with low-grade stenoses, and hence, high competitive flow, were excluded from statistical analysis.

The etiology of graft failure due to competitive flow has not been thoroughly investigated. Results of our study confirm previous thoughts on the deleterious effects of competitive flow on graft failure [14, 16-19, 21, 22]. Wall shear stress is a major determinant of endothelial function [2-6]. A decrease in WSS may induce endothelial dysfunction leading to intimal hyperplasia, typically seen in vein grafts, and to graft atherosclerosis and failure [24]..

The "string phenomenon" sometimes observed in LIMA grafts may also be the result of an endothelial response to a low WSS due to very high competitive flow in the graft distal to non-significant stenosis. The WSS impact on endothelial cells contributes to vessel homeostasis and lumen dimension, both acute and chronic [5, 25]. Competitive flow leads to lower and disturbed graft flow and, hence, lower and oscillatory WSS in the LIMA graft, which may induce the LIMA graft to narrow its lumen to maintain its WSS within certain limits. This response is in line with a study by Gaudino et al., who found that chronic competitive flow did not affect the mid-term patency of mammary grafts but did reduce the graft diameter [26]. The rate of occurrence of the string phenomenon is still controversial, as is its role in relation to the failure of the LIMA graft [14, 19, 27]. Nevertheless, most studies on graft patency and competitive flow show better long-term patency of grafts when coronaries with severe stenoses are bypassed, compared to grafts placed distal to non-significant stenoses [14, 16-19, 21, 22]. Other arterial grafts, such as the radial and gastroepiploic artery, are less tolerant than vein grafts to competitive flow [28].

Unfortunately the assessment of competitive flow due to a non-critical coronary stenosis is quite difficult in clinical practice because grading of a coronary lesion is generally carried out by angiography. Conventional angiography has some pitfalls for the assessment of coronary stenosis severity [29]. Coronary stenoses from 40 to 90% may produce competitive flow (i.e., reduced flow on exertion, but unchanged resting flow) [30]. The combination of competitive flow from the coronary artery and the flow from the graft will characterize the overall flow pattern and, consequently, the WSS distribution. Fractional flow reserve and intravascular ultrasound are two established methods for the functional and geometric evaluation of stenosis, respectively. They are particularly useful for the reliable scoring of coronary stenoses of moderate severity and, thus, are the tools of choice when interventions on coronary lesions are considered.

Computational fluid dynamics is a well-established tool for the recreation of flow fields existing in complex geometries of pulsatile flow conditions. The accuracy of a CFD model is, however, highly dependent on the quality of geometry and boundary conditions used. Our high-resolution 3-D model together with simultaneous transit-time flow measurements provides excellent conditions for CFD simulation. As this is currently not possible to achieve in patients, a porcine model was used. The accuracy of the results was qualitatively confirmed by comparing observed flow conditions from color-Doppler ultrasound with the simulated flow fields as given in Figure 3. Although our CFD model is a snapshot of the flow condition in a single LIMA-LAD anastomosis, the

mapping of the WSS and OSI may improve the understanding of the patho-physiology of graft performance and failure. We believe this technology will become more important in hemodynamic analysis as computers and CFD software continues to develop.

Limitations of this study include a difficulty in generalizing our findings to every patient and describing the detailed characteristics of the flow in every coronary bypass anastomosis due to large variation in the anatomic structure of coronary arteries. Other limitations are related to the CFD model. First, the geometrical model was simplified as minor branches were removed, leaving the five major left: this simplification could have affected the flow. Second, Newtonian rheology, non-slip conditions and rigid walls were assumed in the CFD simulations. Third, the flow into the small branches could not be measured, but was calculated based on the dimensions of the vessels. Fourth, the pig had normal coronary arteries with good run-off and no collateral flow, unlike the conditions in patients with severe coronary disease.

In conclusion, CFD carried out in a 3-D porcine model, showed that the WSS was markedly decreased and increasingly oscillatory in the anastomosis and in the LIMA graft when high competitive flow from a non-significant proximal coronary stenosis is present. Wall shear stress that developed in the LIMA graft and anastomosis by partial competitive flow from a significant proximal stenosis, however, was comparable to that the in no-competitive flow condition. On clinical grounds, the long-term patency of the LIMA graft may be satisfactory when this conduit is grafted to a coronary vessel with a significant stenosis. On the other hand, low and oscillatory WSS caused by a high competitive flow due to a non-significant proximal stenosis may more likely lead to graft failure.

Acknowledgments
We acknowledge Frank Saeys and Marloes De Witte for their help with the CFD simulations.

Sources of Funding
The Norwegian University of Science and Technology, Trondheim, Norway

Disclosures
Medi-Stim ASA, Norway, provided financial support for equipment and disposables.

Reference List

(1) John LCH. Biomechanics of Coronary Artery and Bypass Graft Disease: Potential New Approaches. *The Annals of Thoracic Surgery* 2009;87:331-338.

(2) Stone PH, Coskun AU, Kinlay S, Popma JJ, Sonka M, Wahle A, Yeghiazarians Y, Maynard C, Kuntz RE, Feldman CL. Regions of low endothelial shear stress are the sites where coronary plaque progresses and vascular remodelling occurs in humans: an in vivo serial study. *Eur Heart J* 2007;28:705-710.

(3) Chatzizisis YS, Coskun AU, Jonas M, Edelman ER, Feldman CL, Stone PH. Role of Endothelial Shear Stress in the Natural History of Coronary Atherosclerosis and Vascular Remodeling: Molecular, Cellular, and Vascular Behavior. *Journal of the American College of Cardiology* 2007;49:2379-2393.

(4) Davies PF. Hemodynamic shear stress and the endothelium in cardiovascular pathophysiology. *Nat Clin Pract Cardiovasc Med* 2009;6:16-26.

(5) Kassab GS, Navia JA. Biomechanical considerations in the design of graft: the homeostasis hypothesis. *Annu Rev Biomed Eng* 2006;8:499-535.

(6) Malek AM, Alper S, Izumo S. Hemodynamic shear stress and its role in atherosclerosis. *JAMA* 1999;282:2035-2042.

(7) Wilson PW. Established risk factors and coronary artery disease: the Framingham Study. *Am J Hypertens* 1994;7:7S-12S.

(8) Feldman CL, Ilegbusi OJ, Hu Z, Nesto R, Waxman S, Stone PH. Determination of in vivo velocity and endothelial shear stress patterns with phasic flow in human coronary arteries: A methodology to predict progression of coronary atherosclerosis. *American Heart Journal* 2002;143:931-939.

(9) Asakura T, Karino T. Flow patterns and spatial distribution of atherosclerotic lesions in human coronary arteries. *Circ Res* 1990;66:1045-1066.

(10) Fukumoto Y, Hiro T, Fujii T, Hashimoto G, Fujimura T, Yamada J, Okamura T, Matsuzaki M. Localized elevation of shear stress is related to coronary plaque rupture: a 3-dimensional intravascular ultrasound study with in-vivo color mapping of shear stress distribution. *J Am Coll Cardiol* 2008;51:645-650.

(11) Frauenfelder T, Boutsianis E, Schertler T, Husmann L, Leschka S, Poulikakos D, Marincek B, Alkadhi H. Flow and wall shear stress in end-to-side and side-to-side anastomosis of venous coronary artery bypass grafts. *Biomed Eng Online* 2007;6:35.

(12) Boutsianis E, Dave H, Frauenfelder T, Poulikakos D, Wildermuth S, Turina M, Ventikos Y, Zund G. Computational simulation of intracoronary flow based on real coronary geometry. *Eur J Cardiothorac Surg* 2004;26:248-256.

(13) Nwasokwa ON. Coronary Artery Bypass Graft Disease. *Annals of Internal Medicine* 1995;123:528-533.

(14) Bezon E, Choplain JN, Maguid YA, Aziz A, Barra JA. Failure of internal thoracic artery grafts: conclusions from coronary angiography mid-term follow-up. *The Annals of Thoracic Surgery* 2003;76:754-759.

(15) Berger A, MacCarthy PA, Siebert U, Carlier S, Wijns W, Heyndrickx G, Bartunek J, Vanermen H, De Bruyne B. Long-Term Patency of Internal Mammary Artery Bypass Grafts: Relationship With Preoperative Severity of the Native Coronary Artery Stenosis. *Circulation* 2004;110:II-36.

(16) Nakajima H, Kobayashi J, Funatsu T, Shimahara Y, Kawamura M, Kawamura A, Yagihara T, Kitamura S. Predictive factors for the intermediate-term patency of arterial grafts in aorta no-touch off-pump coronary revascularization. *European Journal of Cardio-Thoracic Surgery* 2007;32:711-717.

(17) Sabik JF, Blackstone EH. Coronary artery bypass graft patency and competitive flow. *J Am Coll Cardiol* 2008;51:126-128.

(18) Kawamura M, Nakajima H, Kobayashi J, Funatsu T, Otsuka Y, Yagihara T, Kitamura S. Patency rate of the internal thoracic artery to the left anterior descending artery bypass is reduced by competitive flow from the concomitant saphenous vein graft in the left coronary artery. *European Journal of Cardio-Thoracic Surgery* 2008;34:833-838.

(19) Villareal RP, Mathur VS. The string phenomenon: an important cause of internal mammary artery graft failure. *Tex Heart Inst J* 2000;27:346-349.

(20) Ku DN, Giddens DP, Zarins CK, Glagov S. Pulsatile flow and atherosclerosis in the human carotid bifurcation. Positive correlation between plaque location and low oscillating shear stress. *Arteriosclerosis* 1985;5:293-302.

(21) Hirotani T, Kameda T, Shirota S, Nakao Y. An evaluation of the intraoperative transit time measurements of coronary bypass flow. *Eur J Cardiothorac Surg* 2001;19:848-852.

(22) Botman CJ, Schonberger J, Koolen S, Penn O, Botman H, Dib N, Eeckhout E, Pijls N. Does Stenosis Severity of Native Vessels Influence Bypass Graft Patency? A Prospective Fractional Flow Reserve-Guided Study. *The Annals of Thoracic Surgery* 2007;83:2093-2097.

(23) Shah PJ, Durairaj M, Gordon I, Fuller J, Rosalion A, Seevanayagam S, Tatoulis J, Buxton BF. Factors affecting patency of internal thoracic artery graft: clinical and angiographic study in 1434 symptomatic patients operated between 1982 and 2002. *European Journal of Cardio-Thoracic Surgery* 2004;26:118-124.

(24) Slager CJ, Wentzel JJ, Gijsen FJ, Schuurbiers JC, van der Wal AC, van der Steen AF, Serruys PW. The role of shear stress in the generation of rupture-prone vulnerable plaques. *Nat Clin Pract Cardiovasc Med* 2005;2:401-407.

(25) Gusic RJ, Myung R, Petko M, Gaynor JW, Gooch KJ. Shear stress and pressure modulate saphenous vein remodeling ex vivo. *J Biomech* 2005;38:1760-1769.

(26) Gaudino M, Alessandrini F, Nasso G, Bruno P, Manzoli A, Possati G. Severity of coronary artery stenosis at preoperative angiography and midterm mammary graft status. *The Annals of Thoracic Surgery* 2002;74:119-121.

(27) Seki T, Kitamura S, Kawachi K, Morita R, Kawata T, Mizuguchi K, Hasegawa J, Kameda Y, Yoshida Y. A quantitative study of postoperative luminal narrowing of the internal thoracic artery graft in coronary artery bypass surgery. *J Thorac Cardiovasc Surg* 1992;104:1532-1538.

(28) Glineur D, D'hoore W, El KG, Sondji S, Kalscheuer G, Funken JC, Rubay J, Poncelet A, Astarci P, Verhelst R, Noirhomme P, Hanet C. Angiographic predictors of 6-month patency of bypass grafts implanted to the right coronary artery a prospective randomized comparison of gastroepiploic artery and saphenous vein grafts. *J Am Coll Cardiol* 2008;51:120-125.

(29) Lindstaedt M, Spiecker M, Perings C, Lawo T, Yazar A, Holland-Letz T, Muegge A, Bojara W, Germing A. How good are experienced interventional cardiologists at predicting the functional significance of intermediate or equivocal left main coronary artery stenoses? *International Journal of Cardiology* 2007;120:254-261.

(30) Gould KL, Lipscomb K, Hamilton GW. Physiologic basis for assessing critical coronary stenosis. Instantaneous flow response and regional distribution during coronary hyperemia as measures of coronary flow reserve. *Am J Cardiol* 1974;33:87-94.

Figure 1

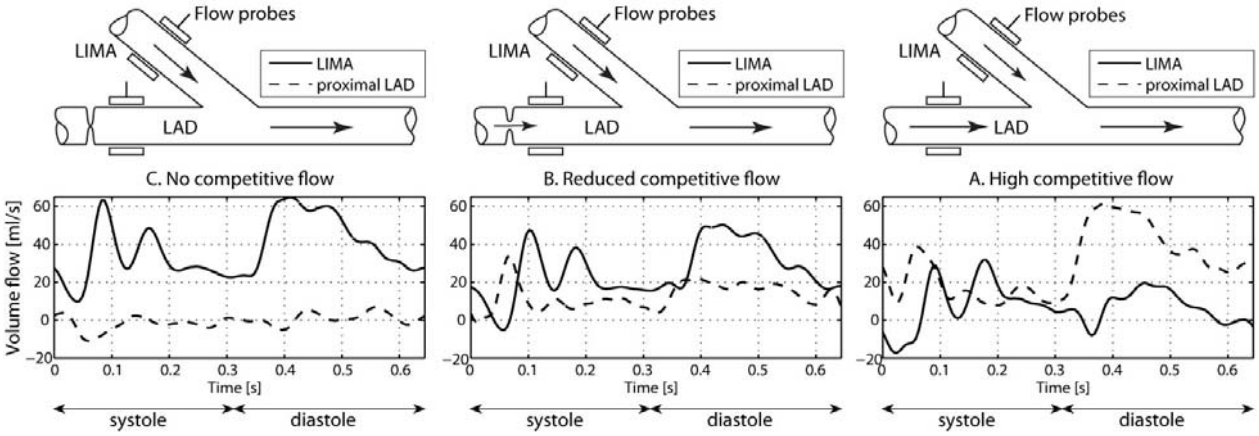

Legend: Schematic layout of the three flow conditions. The upper panels show the three different competitive flow conditions. The LAD flow was adjusted with a vascular occluder around the proximal LAD. Lower panels show the blood flow in the LIMA and LAD.
(A) The proximal LAD is totally occluded, simulating an ideal situation with no competitive flow;
(B) Partial occlusion of the LAD; competitive flow is half of the LAD flow in condition C, simulating a situation with significant coronary stenosis;
(C) No occlusion of the proximal LAD: high competitive flow, simulating non-significant coronary stenosis.

Figure 2

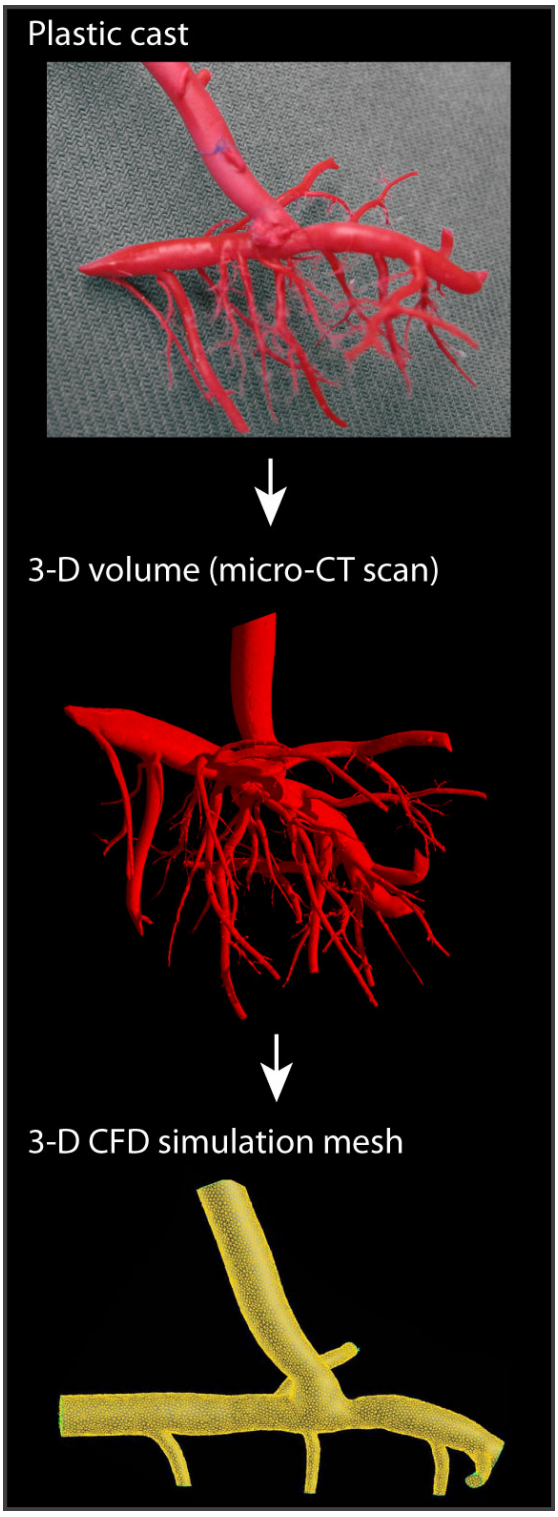

Legend: The creation of a 3-D computer model was a three-stage process: 1) A plastic cast was made of the anastomosis. 2) The 3-D volume was reconstructed using micro-CT with a resolution of 17 μm. 3) The final CFD simulation mesh was extracted from the 3-D volume and simplified by removing the smaller septals and diagonals.

Figure 3

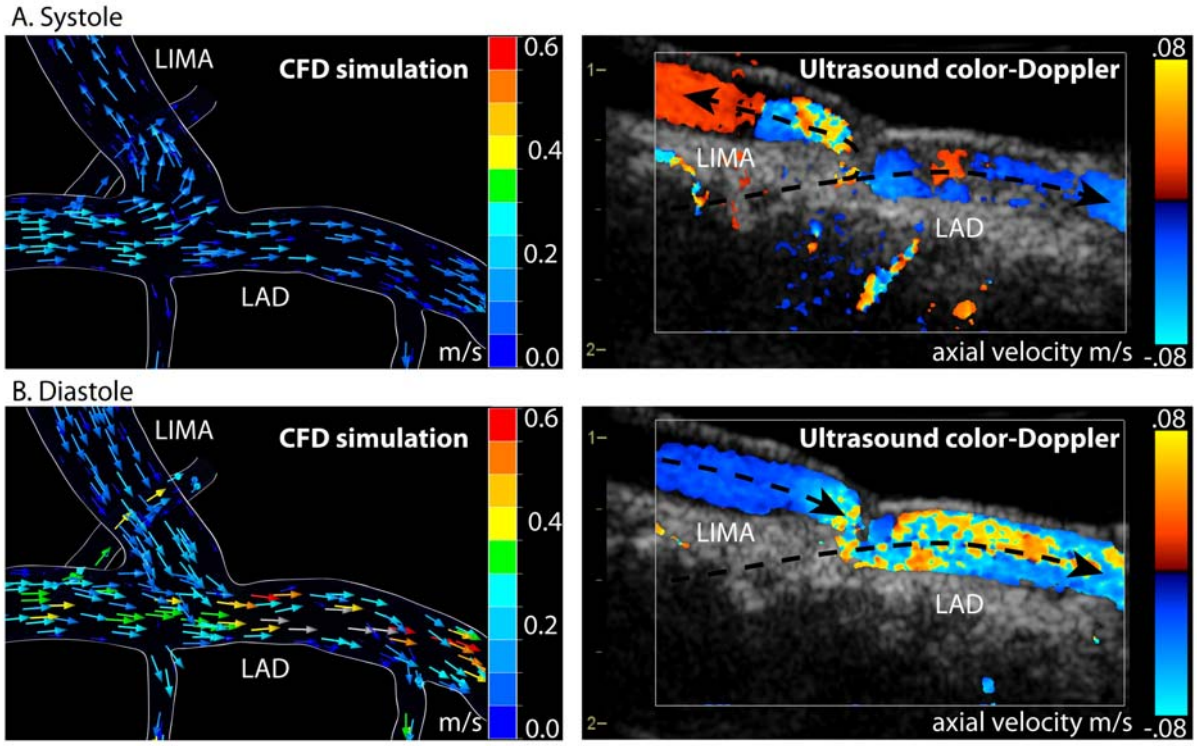

Legend: A qualitative comparison of the CFD simulations with ultrasound color Doppler imaging during (A) systole and (B) diastole during high competitive flow. The left columns show the predicted CFD velocity fields indicated by arrows, where the arrow color is given by the velocity vector magnitude. The right columns show color Doppler images from approximately the same time instance, where the color is given by the axial velocity component (i.e. the component parallel to the ultrasound beam). In systole (upper panels), backflow into the LIMA could be observed using color Doppler and was also reproduced by the CFD flow field. In diastole (lower panels), increased flow velocities from the proximal LAD was predicted by CFD, which also was observed using color Doppler. Furthermore, comparing the axial velocity magnitudes, the same range was observed for both color Doppler imaging and CFD.

Figure 4

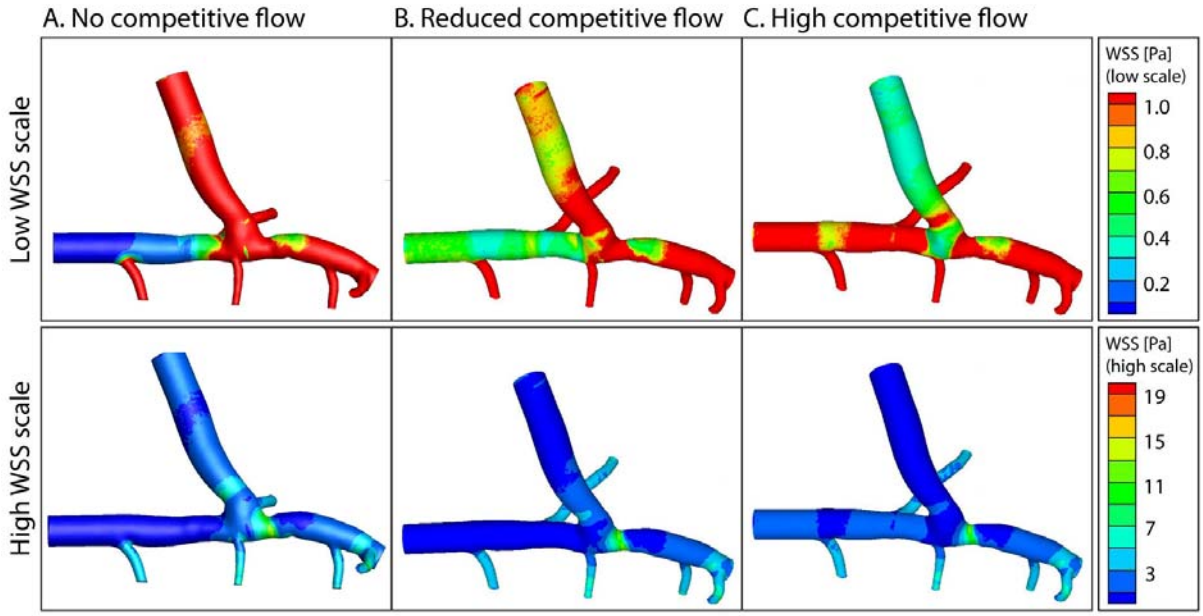

Legend: Time-average distribution of the WSS in the LIMA–LAD model during one cardiac cycle. The upper and lower panels show low and high-scale of WSS, respectively. No competitive flow (A) shows WSS > 1 Pa in the LIMA graft. In comparison, a slightly lower WSS is seen during partial (reduced) competitive flow (B) (0.6 - >1 Pa). Substantially lower WSS in the LIMA graft is seen during full, unaffected competitive flow (C) (0.3 - 0.7 Pa). Elevated WSS levels are shown at the toe of the anastomosis where a moderate narrowing of the vessel lumen had formed.

Figure 5

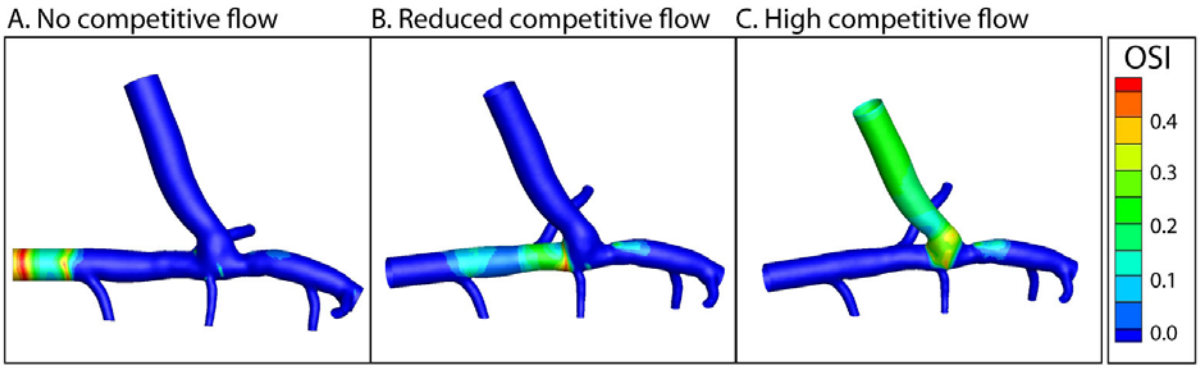

Legend: The oscillatory shear index (OSI) distribution during one cardiac cycle.
No (A) and partial (reduced) (B) competitive flow leads to very low OSI values (<0.05). Higher OSI values (0.15-0.40) are found in the distal LIMA graft and within the anastomosis during high competitive flow (C).

Figure 6

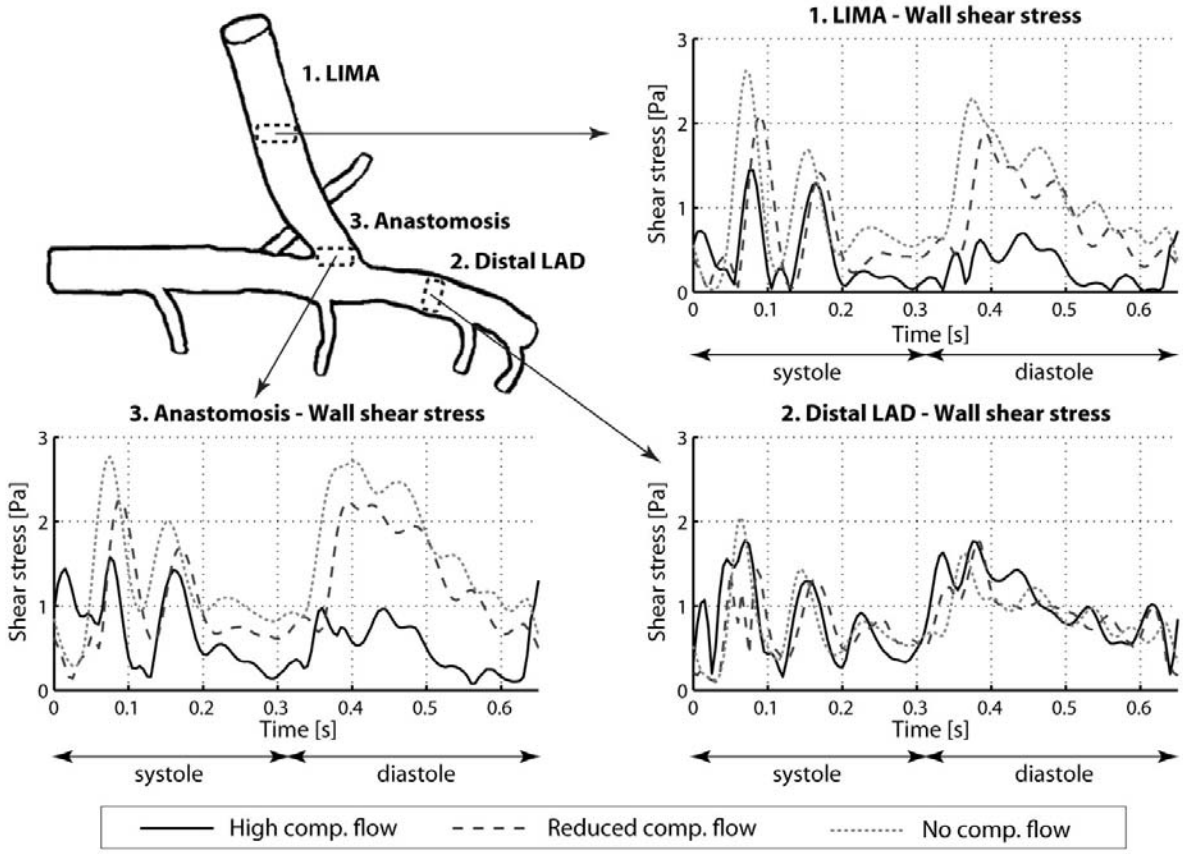

Legend: WSS curves in three different areas: the anastomosis, LIMA and distal LAD. High competitive flow decreases WSS at the anastomosis and in the LIMA. Partial (reduced) competitive flow and no competitive flow produce more comparable WSS curves. Distal LAD is unaffected by competitive flow.